Prediction of dynamic parameters in turning of aluminum metal matrix nano composite by using constitutive models and FEA

M. Madduleti*, P. Venkata Ramaiah

Sri Venkateswara University, Tirupati, India

ABSTRACT

KEYWORDS

Dynamic Parameters,
AMMNC,
Oxley's Model,
JC Model.

The present investigation mainly focused on prediction of cutting parameters in turning of aluminum metal matrix nanocomposite (AMMNC) by using constitutive models based on experimental values. The composite is prepared by reinforcing the multiwall carbon nanotubes (wt. % 2) with aluminum 7075 using stir casting method. The turning experiments are conducted on work material according to Taguchi experimental design (L16) for different speed, feed and depth of cut combinations and the output responses cutting force, thrust force and temperatures are recorded. Afterward, the dynamic parameters such as strain, strain rate, temperature and tool chip interfacial friction are calculated using Oxley's model based on orthogonal experimental values and flow stress is determined by JC model using the values obtained from Oxley's model. Finally, FEM simulations have been performed using 2D-Deform software. The flow stress, temperature, and tool chip interfacial friction are obtained from 2D-Deform software, which is compared with the results obtained from constitutive models and found that comparison is satisfactory.

1. Introduction

Majority of industrial applications of machining are in metals. Although the metal cutting process has resisted theoretical evaluation as a result of its intricacy, the application of these procedures in the commercial world is prevalent. Machining processes are performed on a wide range of equipment tools. Metal cutting operations can be checked out as containing independent input variables, reliant variables, and also independent-dependent interactions or connections. The engineer or machine tool operator has direct control over the input variables as well as can define or pick them when establishing the machining procedure. Transforming is a machining process for generating exterior surfaces of revolution by the action of a reducing device on a rotating workpiece, typically in a lathe. Transforming is the major procedure in a machining sequence discussing in this research work. A lathe is a maker tool which rotates the workpiece on its axis to execute numerous operations such as cutting, knurling, boring, thread reducing and so on with tools that are put on the work item to create an object which has proportion regarding an axis of rotation. Turrets are made use of in woodturning, metalworking, metal rotating, Thermal splashing, parts reclamation, and also glass-working. Aluminum alloys can be machined rapidly as well as financially. As a result of their intricate metallurgical framework, their machining characteristics transcend to those of pure aluminum. The micro-constituents present in aluminum alloys has essential results on machining characteristics.

The literary works study indicates that, in machinability researches investigations, the analytical layout of experiments are used fairly extensively. Statistical design of experiments describes the process of planning the experiment to make sure that the suitable data can be analyzed by statistical techniques, causing valid as well as unbiased verdicts. Design and also techniques such as factorial design, RSM as well as Taguchi methods are now extensively applied instead of one-factor-at-a-time speculative technique which is time-consuming and also excessively high in cost. In the literature study, it appears that enough methodical research work has not been brought out regarding machinability of aluminum alloys such as Al7075/ carbon nanotubes. In the present examination, it has been executed systematically to examine the effects

*Corresponding author,
E-mail: madhubabu56@gmail.com

of all cutting specifications such as feed, cutting rate, as well as the depth of cut on machinability elements during turning on Al7075/MWCNT.

2. Material selection and methods

2.1 Material

The Al7075/ MWCNT composites were used as workpiece material to study machinability aspects in the present investigation. The size of the workpiecesused in the present investigation is 36 mm diameter and 200 mm in length. The chemical composition of aluminum 7075 alloys, physical and mechanical properties of multi-walled carbon nanotube reinforcement are shown in Tables 1 and 2.

2.2 Experimental setup and fabrication

The experimental arrangement for the production of nanocomposite materials is shown in Fig. 1. The setup consists of stir casting equipment, stainless steel stirrer, melting furnace and preheated furnace. The stainless steel stirrer is coated with alumina in order to withstand high temperatures.

Aluminum alloy 7075 was melted in the electric furnace at 750^{0}C and the preheated reinforcements (750^{0}C) and 1wt. % of magnesium gradually included in liquefied metal. The metal mixture underwent mixing for about 15 minutes. After that, the temperature level of the furnace is lowered simultaneously the mixing action was executed on the composite mix until the temperature level goes down to around 590^{0}C. The composite blend was saturated at 590^{0}C for 10 minutes as well as reheated to 750^{0}C and mixing was provided for 2 min (Semi-solid mixing). After that liquefied slurry cascaded into the preheated metallic die. Aluminum matrix composites with weight percentages of MWCNT were made, consisting of 2 wt. %. To determine the flow stresses samples were prepared according to ASTM standards. The microstructure of the composites is carried through SEM, and XRD analysis.

3. Heat Treatment Process

The composite samples were generally heat treated as per T6 process. The samples were solution heat-treated at 450^{0}C for one hour. After that these samples were quenched into pure water. Then finally precipitation treatment was carried out for about 24 hours at 160^{0}C. After completion of the heat treatment process, the samples were cut using wire cut EDM as per ASTM standards.

4. Metallographic Analysis

Microstructures of as-cast, as well as heat-treated metal matrix nanocomposites specimens, were analyzed metallographically. The as-cast specimens were initially cut and positioned. After

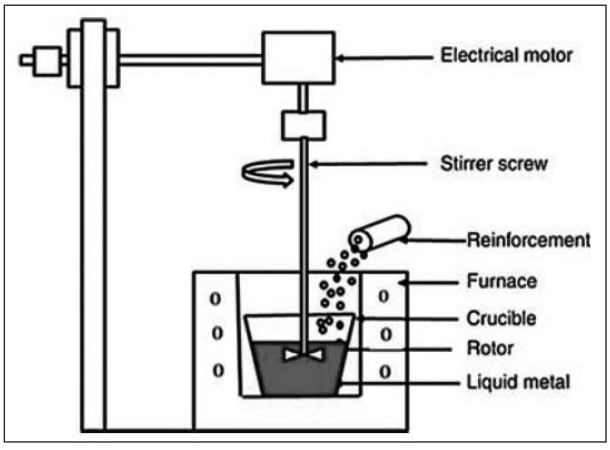

Fig. 1. Stir casting setup.

Table 1
Chemical composition (wt. %) of Al 7075.

Aluminum 7075	Ti	Mn	Si	Cr	Fe	Zn	Ti	Mg	others	Al
Wt.% of composition	0.045	0.04	0.054	0.2	0.21	5.64	0.043	2.2	0.027	Reminder

Table 2
Properties of multi-walled carbon nanotube.

Reinforcement Material	Density (g/cc)	Thermal conductivity (W/m K)	Thermal expansion (10^{-6}/K)	Melting Point temp (^{0}C)	Young's modulus (GPa)
MWCNT	1.9	3000	6.0	2800	450

that these specimens were grinded, polished and etched along with Keller solution that consists of 95% H_2O, 2.5% HNO_3, 1.5% HCl, and 1% HF.

5. Turning Input and Output Process Parameters of Al7075/MWCNT

Turning experiments were conducted on AMMNC cylindrical work piece having a diameter of 36 mm according to Taguchi orthogonal array L16. The cutting conditions employed for turning of AMMNC material are cutting speed, feed and depth of cut at four different levels is shown in Table 3. The responses cutting force, thrust force are measured using lathe tool dynamometer and temperature is measured with temperature gun. Orthogonal cutting test output values are recorded for different speeds, feeds and depth of cuts are shown in the Table 4.

Table 3
Input process parameters for machining of Al7075/MWCNT.

Parameters	Level 1	Level 2	Level 3	Level 4
Speed (rpm)	280	450	710	1120
Feed (mm)	0.2	0.4	0.6	0.8
Depth of cut (mm)	0.2	0.25	0.32	0.36

6. Constitutive Models

The following constitutive models, like Oxley's model, Johnson cook model and Interfacial friction model are used in this present work for predicting the dynamic parameters such as stain, strain rate, Temperature and flow stress at secondary shear zone.

6.1 Oxley's model

Oxley's model is used to predict the process parameters such as stain, strain rate, and Temperature. The description of this model is given in the followings

Strain rate constant proposed by Oxley $l_{AB} = t_u / \sin(\Phi)$ ..... (1)

Shear velocity $V_S = \{v \cos \alpha / [\cos(\Phi - \alpha)]\}$ .... (2)

Table 4
Input and output parameters for Al7075/MWCNT.

S. No	Input parameters			Output parameters		
	Speed (rpm)	Depth of cut (mm)	Feed (mm)	Cutting force (N)	Thrust force (N)	Temperature (^oC)
1	280	0.2	0.2	39.24	9.81	36.8
2	280	0.4	25	88.29	19.62	37.2
3	280	0.6	0.32	137.34	29.43	39.2
4	280	0.8	0.36	176.58	39.24	39.6
5	450	0.2	0.2	39.24	9.81	36.8
6	450	0.4	25	68.67	9.81	38.8
7	450	0.6	0.32	78.48	19.62	37
8	450	0.8	0.36	137.34	19.62	36.5
9	710	0.2	0.2	49.05	9.81	36.8
10	710	0.4	25	78.48	9.81	37.4
11	710	0.6	0.32	137.34	19.62	39
12	710	0.8	0.36	186.39	39.24	39.8
13	1120	0.2	0.2	39.24	9.81	36.7
14	1120	0.4	25	88.29	19.62	36.8
15	1120	0.6	0.32	127.53	19.62	37
16	1120	0.8	0.36	166.77	29.43	38.3

γ_{AB} is the Effective shear strain rate along shear plane AB

$$\gamma_{AB} = \{ \cos\alpha / [2\sin\Phi \cos(\Phi - \alpha)] \} \quad \text{..... (3)}$$

$$\text{Shear angle } \Phi = \tan^{-1}\{ [(tu/tc)\cos\alpha] /[1- (tu/tc) \sin\alpha] \} \quad \text{..... (4)}$$

k_{AB} is the Shear flow stress along shear plane AB

$$k_{AB} = [F_S \sin\Phi / (tu\ w)] \quad \text{..... (5)}$$

$$\text{Shear force } F_S = [F_C\cos\Phi - F_T\sin\Phi] \quad \text{..... (6)}$$

$$T_{AB} = T_0 + \{[(1-\beta) F_S\cos\alpha]/[\rho Stuw\cos(\Phi - \alpha)]\} \quad \text{.... (7)}$$

R_T =Non-dimensional thermal number

$$R_T = [\rho SVtu / K] \quad \text{..... (8)}$$

$$\text{Flow stress } \sigma_{AB} = \sqrt{3}k_{AB} \quad \text{..... (9)}$$

$$\text{Strain along the Shear plane AB, } \varepsilon_{AB} = (\gamma_{AB} / \sqrt{3}) \quad \text{..... (10)}$$

$$\text{Strain rate along the Shear plane AB } \dot{\varepsilon}_{AB} = (\dot{\gamma}_{AB} /\sqrt{3}) \quad \text{..... (11)}$$

The orthogonal cutting test values are given as input to Oxley's model and results are given in Table.5

6.2 Johnson cook model

The Johnson-Cook constitutive model Eq. (12), gives the flow stress as the product of strain, strain rate and temperature effects; i.e. work hardening, strain-rate hardening, and thermal softening.

$$\sigma = [A+B\varepsilon^n] [1+C\ln(\dot{\varepsilon}/\varepsilon_0)] \{1- [(T - T_0)/(Tm - T_0)]^m\} \quad \text{..... (12)}$$

In the above equation, the parameter A is the initial yield strength of the material at room temperature. The equivalent plastic strain rate ε0 is normalized with a reference strain rate ε̇0. T0 is room temperature, and Tm is the melting temperature of the material. While the parameter n takes into account the strain hardening effect, the parameter m takes into account the thermal softening effect and C represents strain rate sensitivity. The constants of Johnson-cook constitutive model from SHPB test are given in Table 6.

Table 5
Oxley's model values.

S.No	ε_{AB}	$\dot{\varepsilon}AB$ (s^{-1})	T_{AB} (^0C)	k_{AB} (N/mm^2)
1	0.90	1080.38	42.67	788.63
2	0.62	1157.17	43.19	813.85
3	0.77	644.71	40.78	510.58
4	1.36	697.56	41.10	566.29
5	0.93	699.92	39.52	434.21
6	0.97	500.90	39.09	1092.9
7	1.50	632.90	37.51	306.18
8	0.84	779.83	38.74	402.20
9	0.45	1269.14	37.62	402.03
10	0.82	1922.31	39.04	416.52
11	0.60	1918.99	40.02	497.89
12	0.64	1310.18	38.57	428.95
13	1.65	925.35	38.49	269.89
14	0.96	1073.68	37.33	235.24
15	0.59	1490.56	40.37	487.46
16	1.06	1450.27	39.02	363.97

Table 6
Constants of Johnson-cook constitutive model from SHPB test.

JC Constants	AMMNC
A[MPa]	535
B[MPa]	579
C	0.018
n	0.74
m	1.64
Tm[K]	900

Table 7
Johnson cook model values.

S.No	Speed (rpm)	Depth of cut (mm)	Feed (mm)	Flow stress (N/mm^2)
1	280	0.2	0.2	1365.95
2	280	0.4	25	1209.63
3	280	0.6	0.32	884.35
4	280	0.8	0.36	980.84
5	450	0.2	0.2	752.07
6	450	0.4	25	893.06
7	450	0.6	0.32	530.32
8	450	0.8	0.36	696.63
9	710	0.2	0.2	696.34
10	710	0.4	25	721.43
11	710	0.6	0.32	862.37
12	710	0.8	0.36	742.96
13	1120	0.2	0.2	467.09
14	1120	0.4	25	407.44
15	1120	0.6	0.32	844.30
16	1120	0.8	0.36	630.41

Johnson cook model is used for determining flow stress based on Oxley's model values and JC constants. These results are shown in Table 7.

6.3 Interfacial friction model

The tool chip interfacial friction model is a mathematical constitutive model and is used for predicting the tool chip interfacial friction at secondary shear zone. The Interfacial friction Model are given in Table 8.

$\mu e = kchip / \sigma_N (l_p)$ ..... (13)

$\sigma N(x) = \sigma N\ max\ [1- (x / lc)^a$ ..... (14)

$$k_{chip} = \frac{F_F}{w\,lp + \frac{w}{\sigma_N(l_p)} \int_{lp}^{lc} \sigma_N(x)\,dx}$$ ..... (15)

$lp = (\delta t_C) / \sin(\phi - \alpha)$ ..... (16)

$F_N = F_C \cos\alpha - F_T \sin\alpha$ ..... (17)

Table 8
Interfacial friction model values.

S. No	FN Normal force component (N)	kchip Shear flow stress in the chip (N/mm^2)	μe co-efficient of friction
1	15.062	58.64	0.67
2	16.684	87.62	0.71
3	28.868	169.75	0.93
4	30.24	149.80	0.74
5	11.586	98.149	1.689
6	13.209	213.48	1.715
7	27.286	180.475	0.964
8	32.027	224.39	0.884
9	23.347	27.79	0.945
10	22.526	189.49	0.498
11	27.113	251.978	0.873
12	30.878	201.305	0.93
13	8.632	178.99	0.95
14	15.178	164.8334	0.895
15	24.679	227.55	1.20
16	34.99	206.64	0.72

$F_F = F_C \sin\alpha + F_T \cos\alpha$ ..... (18)

7. Finite Element Analysis of Orthogonal Cutting

In the present work FEA of metal cutting has been performed by 2D-Deform software. DEFORM-2D is a Finite Element Method (FEM) based process simulation system designed to analyze three dimensional (2D) various metal cutting processes. It provides vital information about the material and thermal flow during the cutting process to facilitate the design of products and required tooling. DEFORM-2D has been used to analyze turning, milling, finishing and many other metal cutting processes.

7.1 Simulation of turning of AMMNC with tungsten carbide tool

Simulations have been performed using 2D-Deform software at different cutting conditions on workpiece material as in the following sections.

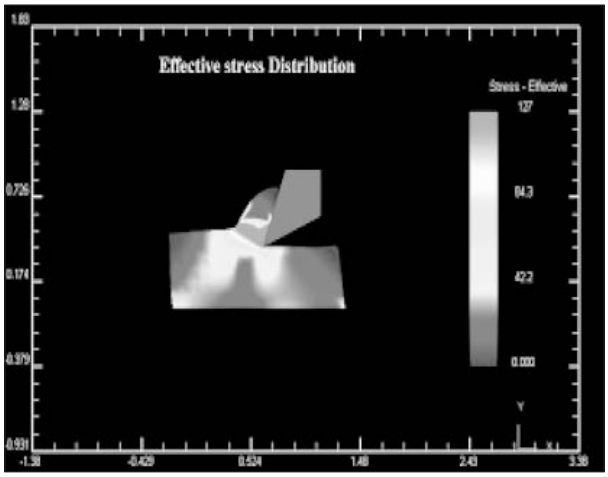

Fig. 2. Flow stress distribution.

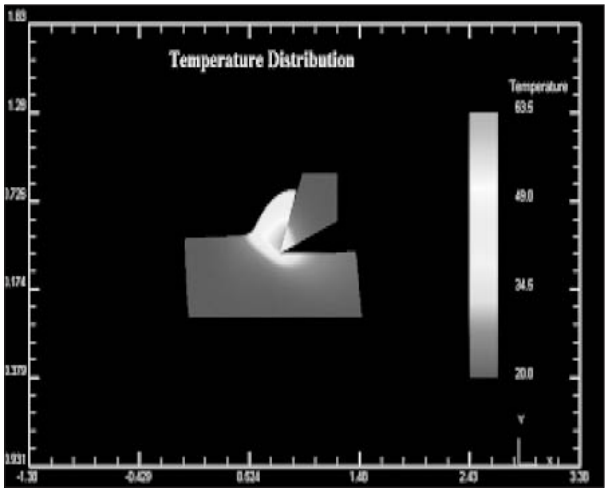

Fig. 3. Temperature distribution.

Analysis on AMMNC at 280 rpm and depth of cut 0.2mm

Input conditions

Machining type	: Turning
Speed	: 280 rpm
Feed	: 0.2mm
Depth of cut	: 0.2mm
Tool material	: Tungsten Carbide
Work piece Material	: AMMNC

Output:

Friction range	: 0.000 to 1.46
Effective Stress	: 0.000 to 127 (N/mm^2)
Temperature	: 20.0 to 63.5 ^{0}C

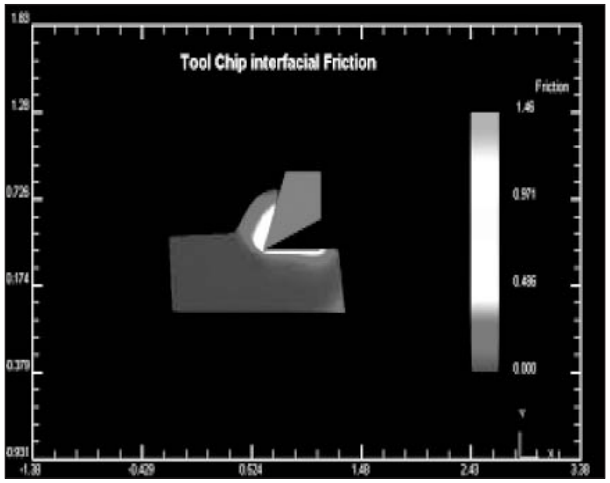

Fig. 4. Tool chip interfacial friction distribution.

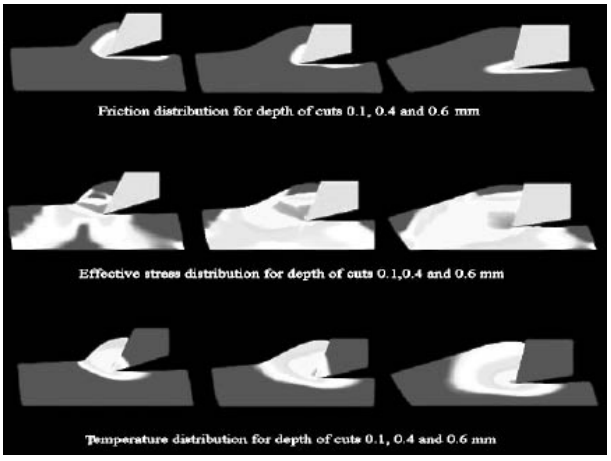

Fig. 5. Flow stress, temperature and friction distribution at various speeds and depth of cuts.

The 2D-Deform software at different cutting conditions on work piece material are shown in Fig (2-5).

The results obtained from 2D-Deform software is shown in Table 9 and the comparison of flow stress, temperature, and friction obtained from Johnson cook model and 2D-Deform software is shown in Table 10, 11, and 12.

7.2 Comparison of Flow stress, temperature and interfacial Friction obtained from constitutive models and 2D-Deform software

By conducting the orthogonal cutting process, the machining responses are taken. These values are substituting Oxley's model to determine the output parameters. The Oxley's output values and Johnson cook constants are substituted in the Johnson cook model, to determine the flow stresses values. The output responses flow stress, temperature and tool chip interfacial friction are recorded from 2D Deform simulation.

Table 9
Results obtained from 2D-Deform software.

Test No	Speed (RPM)	Feed (mm)	Depth of cut (mm)	Flow stress (N/mm^2)	Temperature (^0C)	Friction
1	280	0.2	0.2	1297	39.6	0.85
2	280	0.25	0.4	1234	38.8	0.79
3	280	0.32	0.6	1125	38.3	0.76
4	280	0.36	0.8	1024	37.6	0.72
5	450	0.2	0.2	856	38.5	1.42
6	450	0.25	0.4	784	37.8	1.24
7	450	0.32	0.6	641	36.4	0.87
8	450	0.36	0.8	638	35.8	0.75
9	710	0.2	0.2	658	37.9	0.73
10	710	0.25	0.4	645	36.8	0.69
11	710	0.32	0.6	625	35.4	0.86
12	710	0.36	0.8	621	35.6	0.76
13	1120	0.2	0.2	645	38.6	0.89
14	1120	0.25	0.4	634	37.7	0.84
15	1120	0.32	0.6	628	36.8	0.74
16	1120	0.36	0.8	615	35.4	0.67

Table 10
Flow stress obtained from Johnson cook model and 2D-Deform software.

Test No	Speed (RPM)	Depth of cut (mm)	Flow stress (N/mm^2)	
			JC model	2D-Deform
1	280	0.2	1365.95	1297
2	280	0.4	1409.63	1234
3	280	0.6	884.35	1125
4	280	0.8	980.84	1024
5	450	0.2	752.07	856
6	450	0.4	893.06	784
7	450	0.6	530.32	641
8	450	0.8	696.63	638
9	710	0.2	696.34	658
10	710	0.4	721.43	645
11	710	0.6	862.37	625
12	710	0.8	742.96	621
13	1120	0.2	467.09	645
14	1120	0.4	407.44	634
15	1120	0.6	844.30	628
16	1120	0.8	630.41	615

Table 11
Temperature obtained from Johnson cook model and 2D-deform software.

Test No	Speed (RPM)	Depth of cut (mm)	Temperature (^{0}C)	
			JC model	2D-Deform
1	280	0.2	42.67	39.6
2	280	0.4	43.19	38.8
3	280	0.6	40.78	38.3
4	280	0.8	41.10	37.6
5	450	0.2	39.52	38.5
6	450	0.4	39.09	37.8
7	450	0.6	37.51	36.4
8	450	0.8	38.74	35.8
9	710	0.2	37.62	37.9
10	710	0.4	39.04	36.8
11	710	0.6	40.02	35.4
12	710	0.8	38.57	35.6
13	1120	0.2	38.49	38.6
14	1120	0.4	37.33	37.7
15	1120	0.6	40.37	36.8
16	1120	0.8	39.02	35.4

Table 12
Comparison of interfacial friction obtained from johnson cook model and 2D-deform software.

Test No	Speed (RPM)	Depth of cut (mm)	Interfacial Friction	
			JC model	2D-Deform
1	280	0.2	0.67	0.85
2	280	0.4	0.71	0.79
3	280	0.6	0.93	0.76
4	280	0.8	0.74	0.72
5	450	0.2	1.689	1.42
6	450	0.4	1.715	1.24
7	450	0.6	0.964	0.87
8	450	0.8	0.884	0.75
9	710	0.2	0.945	0.73
10	710	0.4	0.498	0.69
11	710	0.6	0.873	0.86
12	710	0.8	0.93	0.76
13	1120	0.2	0.95	0.89
14	1120	0.4	0.895	0.84
15	1120	0.6	1.20	0.74
16	1120	0.8	0.72	0.67

7.2.1 Flow stress

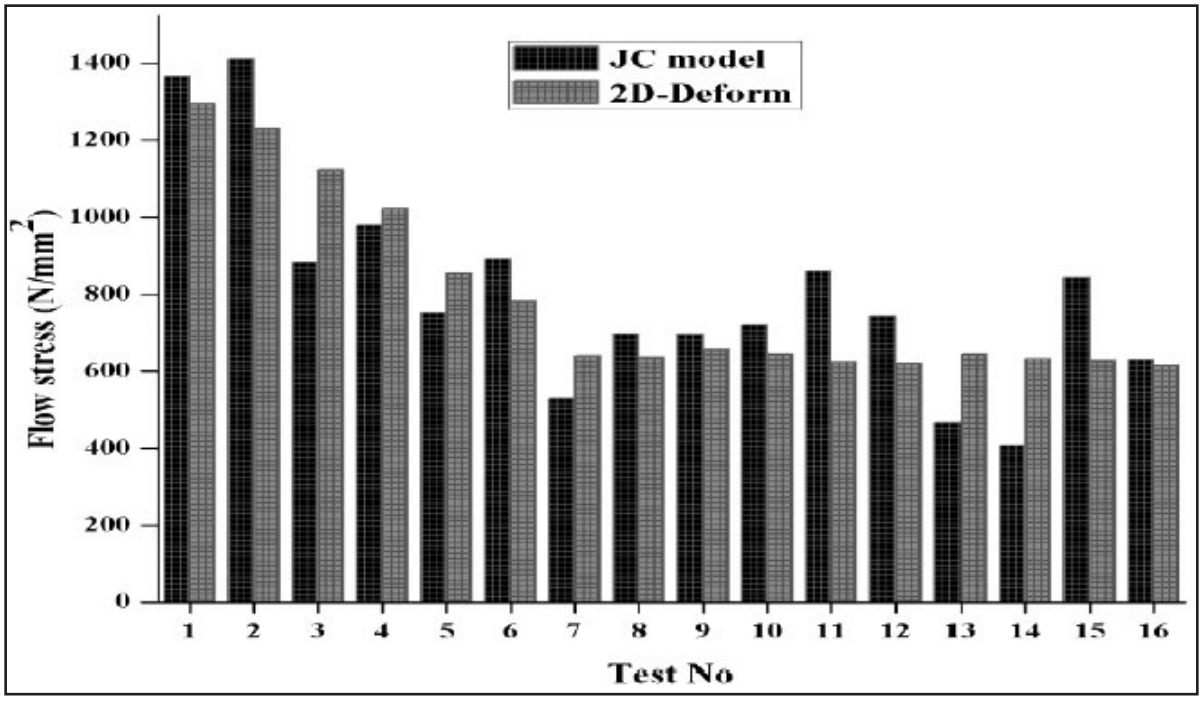

Fig. 6. Flow stress obtained from johnson and 2D-deform.

7.2.2 Temperature

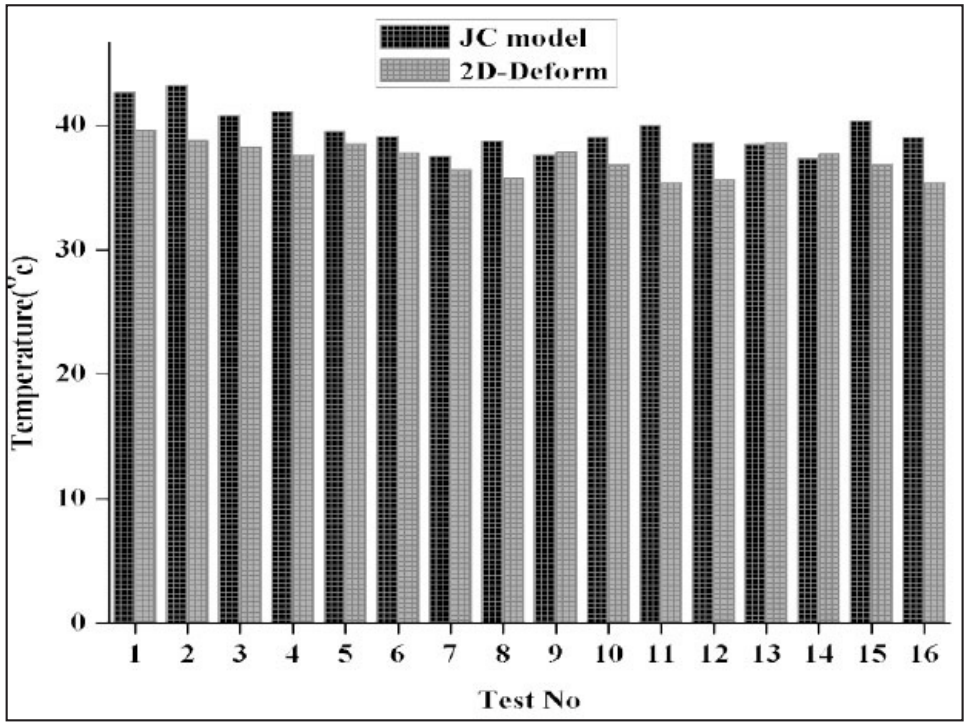

Fig. 7. Temperature obtained from johnson and 2D-deform.

7.2.3 Interfacial friction

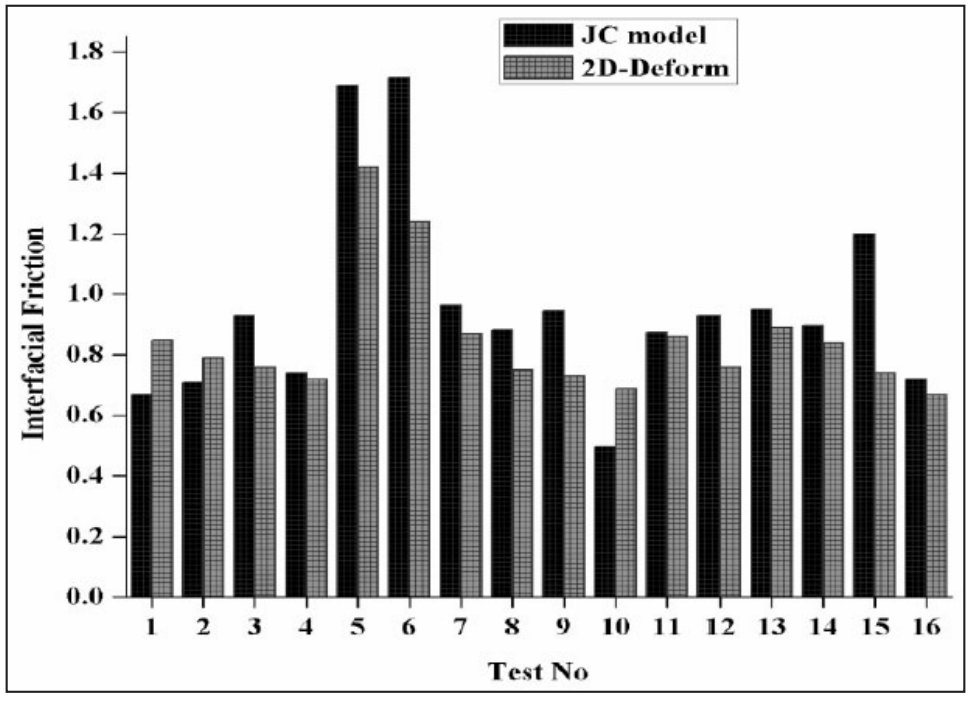

Fig. 8. Friction obtained from johnson and 2D-deform.

Fig (6-8) shows predicted, flow stress, temperature and interfacial friction at secondary zone values for aluminum nanocomposite material are compared with the results obtained from Johnson cook model and 2D-Deform software, and comparison is satisfactory.

8. Results and Discussions

8.1 Effect of speed on flow stress, temperature and friction

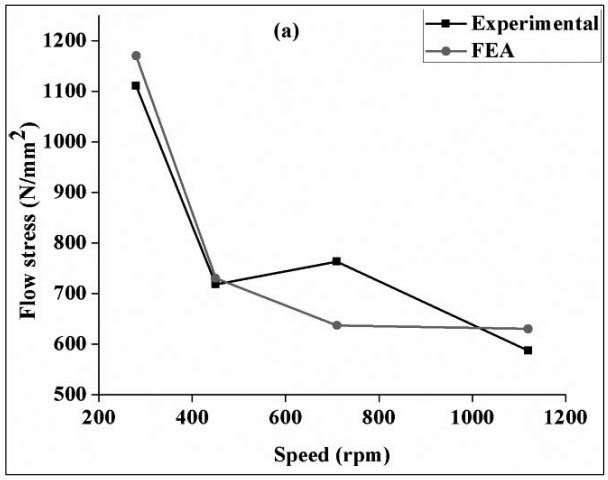

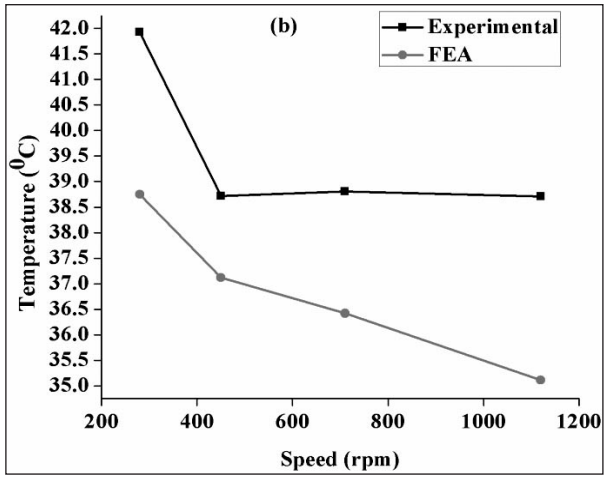

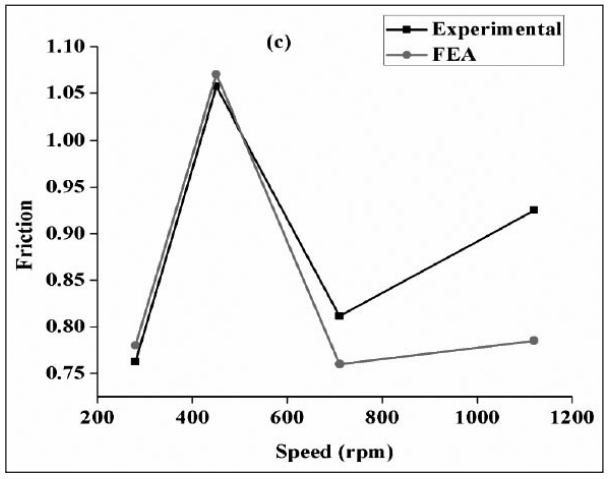

Fig. 9(a-c). Speed vs. flow stress, temperature and friction.

8.2 Effect of feedon flow stress, temperature and friction

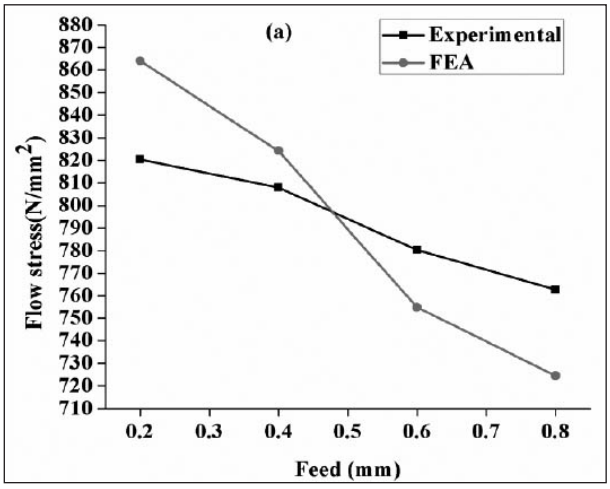

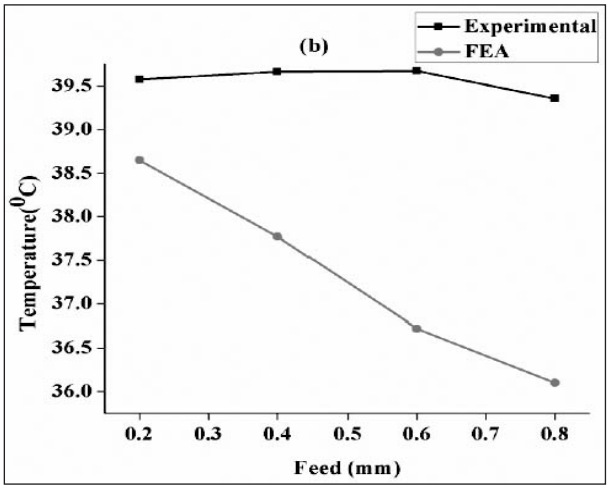

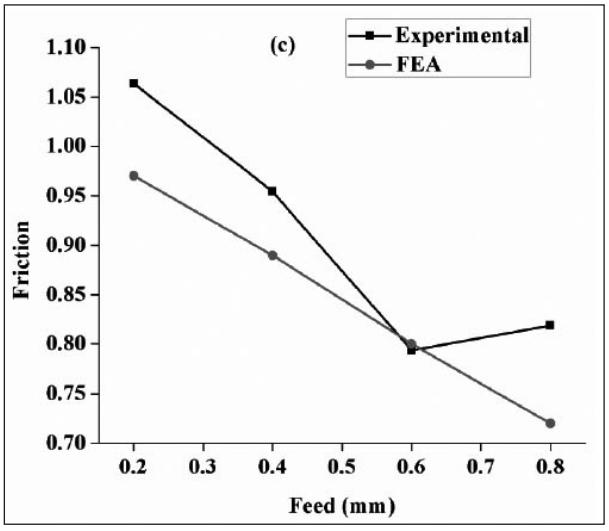

Fig. 10(a-c). Feed vs. flow stress, temperature and friction.

8.3 Effect of depth of cut on flow stress, temperature and friction

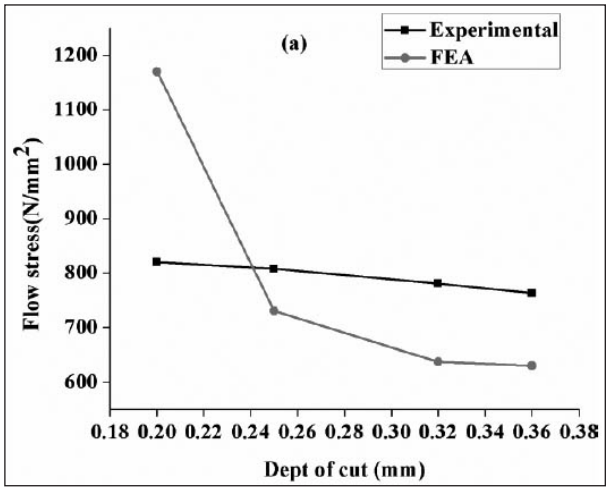

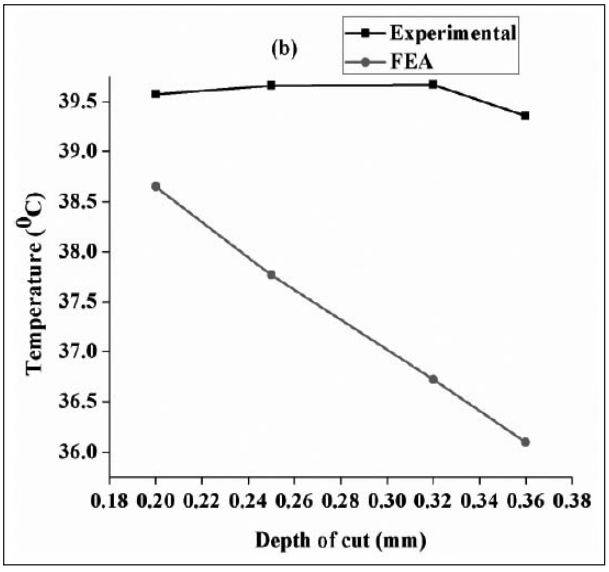

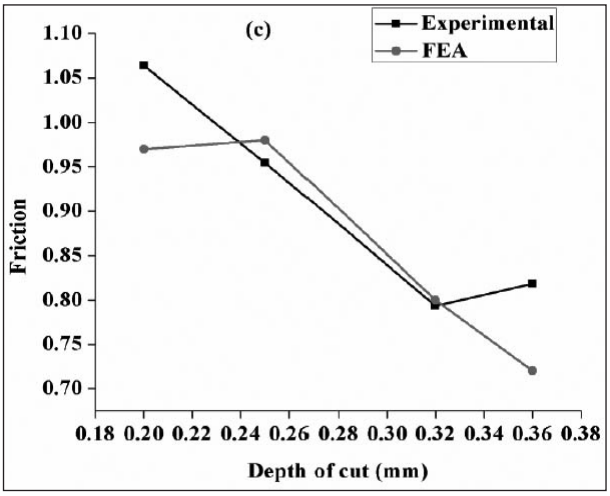

Fig. 11(a-c). Feed vs. flow stress, temperature and friction.

8.4 Optical microscope

Metallographic specimens were cut from the casted composites and were made applying a method particularly produced nano composites. The optical microstructure images at 500X magnifications are shown in Fig 9 (a-b). A Keller's agent was utilized to etch the specimens. Based on microstructural examinations, it is noticed that Al/hybrid nanocomposite possessing cluster fragments and also a few areas are recognized without nano reinforcement inclusions. The main reason is due to high surface tension and poor wetting in between Al 7075 and nano reinforcements. In order to overcome these problems, a mechanical power might be employed homogeneously at the time of the dispersion of nano-reinforcement particulates in the metal matrix nanocomposites.

8.5 SEM analysis

During microstructural analysis, composite samples were sectioned from the cast bars and grinded with emery paper, by using extensive amounts of pure water as a lubricating substance. After that, the specimens were polished by means of a 1µm alumina-powder held in distilled water. Fine polishing was obtained applying the 0.5µm diamond paste as well as etched with Keller's reagent. Nano reinforcement distribution and its morphology in the Al 7075/MWCNT composites and also intrinsic microstructural characteristics were determined by analyzing the specimens in a Scanning Electron Microscope (SEM). Figure 10 (a-b) reveals SEM images of the surface area of the nanocomposites and it shows that the supplements are an ingredient in nanocomposites.

8.6 XRD analysis

The XRD analysis of matrix metal (Al 7075) and MWCNT composites shown in figure 11 respectively. Figure 11 shows the presence of aluminum (Al) and zinc (Zn) in the base alloy. The presence of reinforcement particles along with aluminum, magnesium, copper, and zinc elements are identified in the XRD pattern of the composite. Among these phases, Al_2O_3 and SiC as major phases present in the nanocomposite.

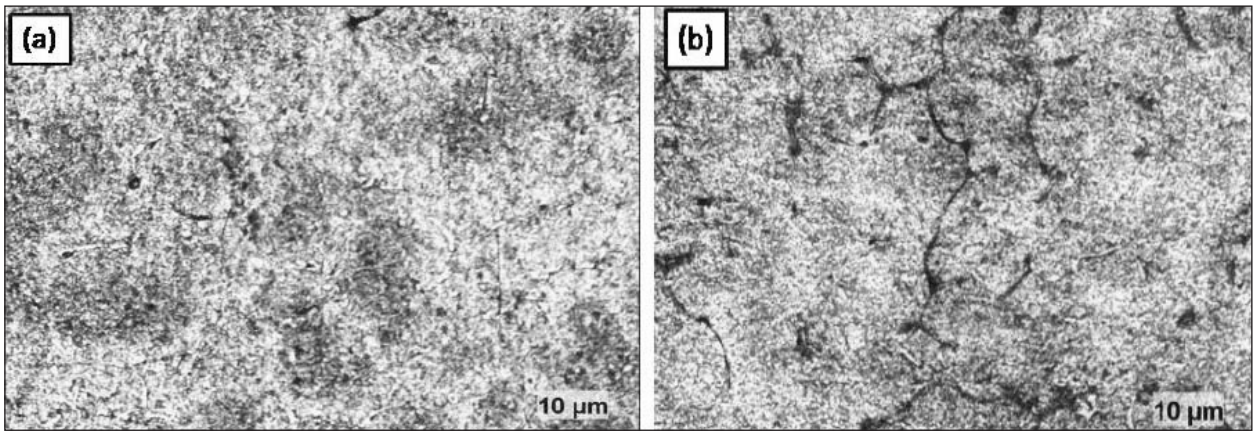

Fig. 12. Optical microscopic images of (a) Al 7075 (b) Al 7075/ 2% MWCNT.

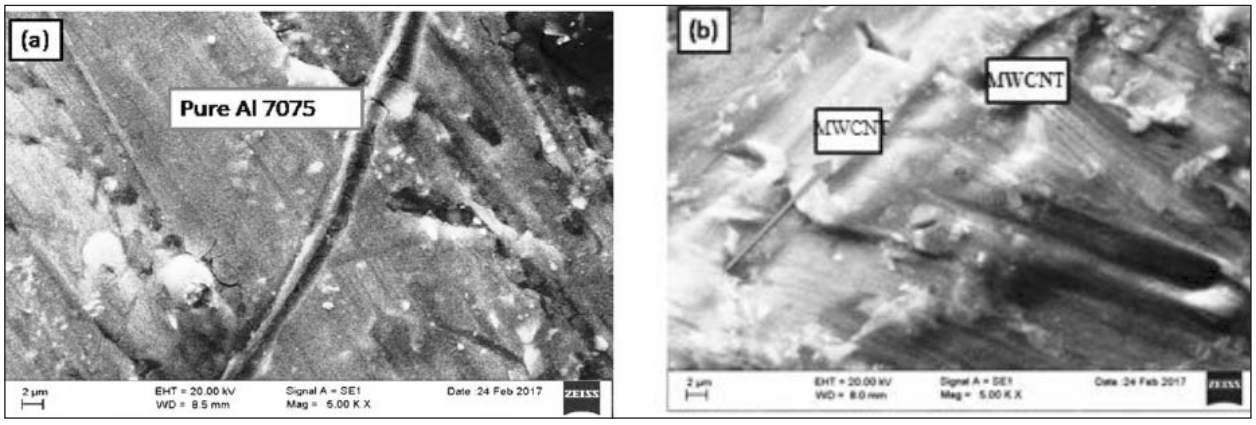

Fig. 13. SEM images of (a) Al 7075 (b) Al 7075/ 2% MWCNT.

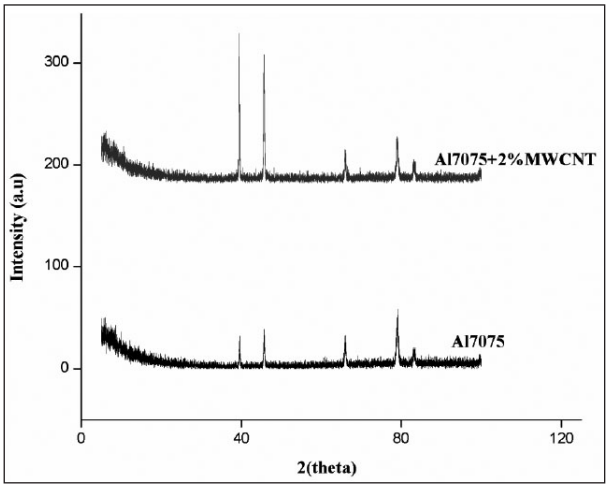

Fig. 14. XRD analysis of (a) Al 7075
(b) Al 7075/ 2% MWCNT.

Conclusions

Present work utilizes an extended metal cutting model developed by Oxley and co-workers and presents an improved methodology to expand the applicability of the Johnson-Cook material model to the cutting conditions. In this work, the dynamic parameters Flow stress, Temperature distribution and Interfacial Friction at secondary shear zone are predicted using Oxley's model. The orthogonal test values speed, feed, depth of cut are given to the 2D-Deform software so to obtain the dynamic parameters. Predicted Flow stress, Temperature and Interfacial friction between tool and chip at secondary zone values for Aluminum nanocomposite material are compared with the results obtained from 2D-Deform software, and comparison is satisfactory.

References

Childs, T. H. C. (1998). *Material property needs in modeling metal machining.* Proceedings of the CIRP International Workshop on Modeling of Machining Operations, Atlanta, Georgia, USA, 193–202.

Dusunceli, N., Colak, O. U., & Filiz, C. (2010). Determination of material parameters of

a viscoplastic model by genetic algorithm. *Materials and Design*, 31(3), 1250-1255. doi:10.1016/j.matdes.2009.09.023

Ghose, J., Sharma, V., Kumar, N., Krishnamurthy, A., Kumar, S., & Botak, Z. (2011). Taguchi fuzzy-based mapping of EDM-machinability of aluminum foam. *Technical Gazette*, 18(4), 595-600.

Gurbuz, H., Kurt, A., Ciftci, I., & Seker, U. (2011). The Influence of Chip Breaker Geometry on Tool Stresses in Turning. *Strojniškivestnik–Journal of Mechanical Engineering*, 57(2), 91-99. doi:10.5545/sv-jme.2009.191

Hamann, J. C., Grolleau, V., & Le Maitre, F. (1996). Machinability improvement of steels at high cutting speeds – the study of tool/work material interaction. *CIRP Annals*, 45, 87–92.

Johnson, G. R., & Cook, W. H. (1983). *A constitutive model and data for metals subjected to large strains, high strain rates, and high temperatures.* Proceedings of the 7th International Symposium on Ballistics. The Hague, The Netherlands, 541–547.

Khan, A. S., Suh, Y. S., & Kazmi, R. (2004). Quasi-static and dynamic loading responses and constitutive modelling of titanium alloys. *International Journal of Plasticity*, 20(12), 2233-2248. doi:10.1016/j.ijplas.2003.06.005

Lee, W. S., & Lin, C. F. (1998). High-temperature deformation behavior of Ti6Al4V alloy evaluated by high strain rate compression tests. *Journal of Materials Processing Technology,* 75(1-3), 127-136. doi:10.1016/S0924-0136(97)00302-6

Lesuer, D. R. (2000). *Experimental investigations of material models for Ti-6Al-4V titanium and 2024-T3 aluminum. Final Report, DOT/FAA/AR-00/2,* US Department of Transportation, Federal Aviation Administration.

Meyer Jr., H. W., & Kleponis, D. S. (2001). Modeling the high strain rate behavior of titanium undergoing ballistic impact and penetration. *International Journal of Impact Engineering,* 26, 509–521.

Motorcu, A. R. (2010). The Optimization of Machining Parameters Using the Taguchi Method for Surface Roughness of AISI 8660 Hardened Alloy Steel. *Strojniškivestnik–Journal of Mechanical Engineering*, 56(6), 391-401.

Mousavi Anijdan, S. H., Madaah-Hosseini, H. R., & Bahrami, A. (2007). Flow stress optimization for 304 stainless steel under cold and warm compression by artificial neural network and genetic algorithm. *Materials, and Design*, 28(2), 609-615. doi:10.1016/j.matdes.2005.07.018

Oxley, P. L. B. (1989). *Mechanics of Machining - an Analytical Approach to Assessing Machinability*. Ellis Horwood Limited.

Özel, T., & Altan, T. (2000). Determination of workpiece flow stress and friction at the chip-tool contact for high-speed cutting. *International Journal of Machine Tools and Manufacture*, 40(1), 133–152.

Ozel, T., & Karpat, Y. (2007). Identification of constitutive material model parameters for high strain rate metal cutting conditions using evolutionary computational algorithms. *Materials and Manufacturing Processes*, 22(5), 659-667. doi:10.1080/10426910701323631

Shatla, M., & Kerk, C. T. (2001). Altan Process modeling in machining - Part I: Determination of flow stress data. *International Journal of Machine Tools and Manufacture*. 41, 1511–1534.

Tay, A. O., Stevenson, M. G., & De Vahl Davis, M. G. G. (1974). Using the finite element method to determine temperature distributions in orthogonal machining. *Proceedings of the Instiution of Mechanical Engineers,* 188(1), 627–638.

Zerilli, F. J., & Armstrong, R. W. (1987). Dislocation-mechanics-based constitutive relations for material dynamics calculations. *Journal of Applied Physics*, 61(5), 1816–1825.

Zorev, N. N. (1963). Inter-Relationship Between Shear Processes Occurring Along Tool Face and Shear Plane in Metal Cutting. *International Research in Production Engineering,* 42–49.

M. Madduleti is a research scholar in Mechanical Engineering Department, Sri Venkateswara University, Tirupati. He is a Graduate in Mechanical Engineering from G. Pulla Reddy Engineering College, Kurnool and M.Tech in Production Engineering from Venkateswara University College of Engineering, Tirupati. He has published more than 10 technical papers In International Journals and Conferences. He has 10 years of teaching experience.

Dr. P. Venkata Ramaiah is Presently working in Mechanical Engineering Department, Sri Venkateswara University, Tirupati. He is a graduate in Mechanical Engineering from Venkateswara University College Engineering, Tirupati and M.Tech in Industrial Engineering From Venkateswara University College of Engineering, Tirupati. He was awarded Ph.D in the year 2007 by Venkateswara University College of Engineering, Tirupati. He has published more than 90 technical papers In International Journals and Conferences. He has 20 years of teaching experience.
(E-mail: pvramaiah@gmail.com)